PERGAMON

International Journal of Heat and Mass Transfer 44 (2001) 939–951

International Journal of HEAT and MASS TRANSFER

www.elsevier.com/locate/ijhmt

# An experimental investigation of film cooling on a convex surface subjected to favourable pressure gradient flow

E. Lutum [a,*], J. von Wolfersdorf [a], K. Semmler [b], J. Dittmar [c], B. Weigand [d]

[a] *ABB ALSTOM POWER, Gas Turbine Development, Heat Transfer Group, Im Segelhof, 5405 Baden-Dättwil, Switzerland*
[b] *ABB ALSTOM POWER, Gas Turbine Development, 5401 Baden, Switzerland*
[c] *Institut für Thermische Strömungsmaschinen, Universität Karlsruhe, Kaiserstraße 12, 76128 Karlsruhe, Germany*
[d] *Institut für Thermodynamik der Luft- und Raumfahrt, Universität Stuttgart, Pfaffenwaldring 31, 70569 Stuttgart, Germany*

Received 1 February 2000; received in revised form 19 April 2000

**Abstract**

The film cooling performance on a convex curved surface subjected to accelerated free-stream flow was investigated. The thermochromic liquid crystals technique was applied to determine adiabatic film cooling effectiveness values and heat transfer coefficients on the test surface. Five different injection geometries, three with cylindrical holes and two with shaped holes were investigated. The experimental results were compared to the results of a previous investigation obtained with constant free-stream velocity to determine the influence of free-stream acceleration. The free-stream acceleration caused decreasing adiabatic film cooling effectiveness values compared to constant free-stream velocity, especially further downstream of the point of injection. For the in-line cylindrical injection configurations, an increase in adiabatic film cooling effectiveness in the near hole region can be obtained for higher blowing rates. It is assumed that this effect is due to the reduced tendency of jet separation in the accelerated free-stream. The influence of the free-stream acceleration on the Stanton number ratio is generally small. 

*Keywords:* Film cooling; Heat transfer; Turbines

## 1. Introduction

In modern gas turbine designs, there is a desire to increase the hot gas temperature for the first stage turbine airfoils. The use of the most efficient cooling technology available is required by this further increased turbine inlet temperature and by the demand of high gas turbine cycle efficiency. The application of film cooling is required at these high turbine inlet temperatures to achieve allowable metal temperature levels. The reduction in thermal strain due to the reduction of external gas temperature achieved by film cooling is another important feature that guarantees component life requirements. Although the development of thermal barrier coating has made good progress during recent years its use is still limited. Film cooling is used in the gas turbine design to reduce the heat load for the turbine airfoils that are exposed to combustion chamber exhaust gases well above allowable material temperature. In the airfoil cooling process, compressor bleed air is introduced into the hollow core of each airfoil and convectively cools the airfoil through several radial coolant passages. In advanced cooling applications, film cooling is used to decrease the external heat load by injecting air through the airfoil surface via several rows of circular or shaped holes to protect the surface against the hot gas.

Film cooling has been extensively studied over the past 30 years and a large body of papers is available in the open literature. Most of these studies concentrate on flat plate configurations with film injection through slots or rows of cylindrical holes. A brief review of film cooling literature that investigated the influence of free-stream pressure gradient is given below. The effect of a free-stream pressure gradient on film cooling performance was studied quite systematically for flat plate

* Corresponding author. Tel.: +41-5648-67064; fax: +41-5648-67359.
*E-mail address:* ewald.lutum@ch.abb.com (E. Lutum).

0017-9310/01/$ - see front matter 
PII: S0017-9310(00)00158-7

**Nomenclature**

| | |
|---|---|
| AR | outlet-to-inlet area ratio of film holes |
| $c_p$ | specific heat at constant pressure |
| $D$ | film hole diameter |
| DR | density ratio between secondary and free-stream fluid, $\rho_c/\rho_\infty$ |
| $h$ | convective heat transfer coefficient |
| $I$ | momentum flux ratio, $(\rho_c U_c^2)/(\rho_\infty U_\infty^2)$ |
| $I_{foil}$ | electrical current applied to the heating foil |
| $K$ | acceleration parameter |
| $L$ | hole length |
| $M$ | blowing rate, $(\rho_c U_c)/(\rho_\infty U_\infty)$ |
| $Ma$ | Mach number |
| $\dot{q}$ | specific heat flux |
| $p$ | static pressure |
| $P$ | total pressure |
| $P$ | lateral spacing of film holes (pitch) |
| $Pr$ | Prandtl number |
| $P/D$ | pitch-to-diameter ratio |
| $R$ | radius of curved test surface |
| $R_{foil}$ | specific resistance of the heating foil |
| $S$ | stream-wise coordinate |
| $St$ | Stanton number |
| $t$ | static temperature |
| $T$ | total temperature |
| $Tu$ | turbulence intensity, $(u'/U_\infty)$ |
| $U$ | mean velocity |

*Greek symbols*

| | |
|---|---|
| $\alpha$ | injection angle relative to the test surface |
| $\beta$ | injection angle relative to the free-stream flow, compound angle |
| $\delta$ | boundary layer thickness |
| $\delta_1$ | boundary layer displacement thickness |
| $\gamma$ | bend angle position |
| $\eta_{ad}$ | adiabatic film cooling effectiveness |
| $\varphi_1$ | extension angle in lateral direction |
| $\varphi_2$ | extension angle in stream-wise direction |
| $\kappa$ | ratio of gas specific heats |
| $\lambda_{Necuron}$ | thermal conductivity of Necuron material |
| $\rho$ | fluid density |
| $\Theta$ | dimensionless wall temperature |

*Subscripts*

| | |
|---|---|
| 0 | without film cooling |
| aw | adiabatic wall |
| c | coolant fluid |
| f | with film cooling |
| inj | injection condition |
| la | lateral averaged |
| r | recovery condition |
| w | wall condition |
| TLC | thermochromic liquid crystals |
| $\infty$ | free-stream fluid |

experiments. Most investigations were performed with favourable pressure gradient flow and fewer results are available for adverse pressure gradient flow situation. Hartnett et al. [1], Seban and Back [2], Carlson and Talmor [3], Escudier and Whitelaw [4] and Pai and Whitelaw [5] investigated the influence of free-stream pressure gradient on adiabatic film cooling effectiveness with slot injection along flat walls. Launder and York [6], Jabbari and Goldstein [7] and Kruse [8] investigated adiabatic film cooling effectiveness on flat plates with injection through cylindrical holes under the influence of free-stream pressure gradient flow. Seban and Back [2] investigated the effect of free-stream pressure gradient on the heat transfer coefficient with film cooling on flat plates with slot injection. Jabbari and Goldstein [7], Hay et al. [9] and Ammari et al. [10] investigated the effect of free-stream pressure gradient on the heat transfer coefficient with film cooling on flat plates with injection through cylindrical holes.

In general the following trends could be observed:

- The free-stream pressure gradient has no significant influence on the film cooling performance on flat surfaces.
- A mild adverse pressure gradient seems to have less effect than a mild favourable pressure gradient. A moderate effect occurs for strong favourable pressure gradients.
- The lateral averaged film cooling effectiveness as well as the lateral averaged heat transfer coefficient is slightly decreased due to favourable pressure gradient flow.
- The lateral spreading of the coolant fluid downstream of injection is reduced by a favourable free-stream pressure gradient.
- The effect of the free-stream pressure gradient on the heat transfer coefficient was less with $CO_2$ injection that with air injection.

Sivrioglu [11] performed two-dimensional boundary layer calculations to study the simultaneous effects of free-stream pressure gradient and wall curvature on adiabatic film cooling effectiveness. For film cooling on flat surfaces the results were similar to those made in the experiments mentioned above. However, a free-stream pressure gradient may have greater influence on adiabatic film cooling effectiveness on curved surfaces than on flat surfaces.

All of the above-mentioned experimental investigations were performed on flat plates with injection through slots or cylindrical holes. Ames [12,13] and Drost and Bölcs [14] conducted film cooling investiga-

tions on airfoil suction and pressure sides with cylindrical hole injection. Airfoil film cooling investigations that investigate effects of shaped hole injection were performed experimentally by Zhang et al. [15] and numerically by Heidmann et al. [16]. Results supplied by these investigations simulate the gas turbine conditions very close and deliver detailed information about the local film cooling performance on airfoil surfaces. However, as the results are derived under simultaneous effects of wall curvature, streamwise pressure gradient and superposition effects of multiple injection rows as typically found for gas turbine applications it is difficult to separate these effects to derive physical models for design applications.

No experimental results obtained with both free-stream pressure gradient and wall curvature that allow a separation of these effects are available in the open literature. Also no data is available for shaped holes for these conditions. The present investigation gives experimental results of adiabatic film cooling effectiveness and heat transfer coefficients obtained on a convex curved surface with free-stream pressure gradient flow. An increased free-stream turbulence intensity of about $Tu_\infty = 6\%$ at the injection location was achieved by means of a turbulence generator. The free-stream boundary conditions were kept constant, but the coolant boundary conditions were systematically varied during these film-cooling experiments. The blowing rates were varied between $0.5 \leqslant M \leqslant 2.0$. The majority of the experiments were conducted with $CO_2$ as coolant fluid, which gave a high-density ratio. Some measurements with air-injection, which gave a low-density ratio, have also been conducted. Film cooling measurements have been performed with five different injection configurations, three with cylindrical and two with shaped holes. The present results will be compared to previous results that have been obtained in the same apparatus but with zero pressure gradient flow.

## 2. Experimental facility and measurement technique

The film cooling test facility was designed to determine film cooling effectiveness and heat transfer increase due to film injection along curved surfaces. The investigation reported here focused on film cooling on a convex surface. Secondary fluid ($CO_2$ or air) was injected through a single row of cylindrical or shaped holes. The multiple narrow-band thermochromic liquid crystal technique was used to determine the local wall temperature distributions along the test surface. A detailed description of the test facility and the injection geometries used during these experiments can be found in [17].

The test section shown in Fig. 1 was built up as a sandwich construction, consisting of a bottom and top

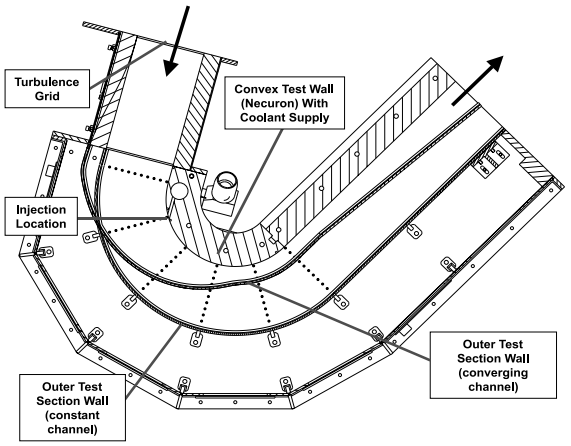


Fig. 1. Convex test section with converging and constant channel ($R/D = 25$).

plate and the inner and outer test section walls. The material of the curved inner wall was Necuron, a low conductive polyurethane based material with a thermal conductivity of $\lambda_{\text{Necuron}} = 0.1$ W/(m K). This wall was segmented into three parts where the middle part contains the injection configuration. Different film injection configurations could be installed by changing this middle segment. The outer test section wall consisted of a polycarbonate plate of 5 mm thickness. Polycarbonate is a polyester-based material, similar to plexiglas, with good mechanical and optical properties. This thin polycarbonate wall was shaped by several flexible fixations at bend angle position of $\gamma = 0°$, 30°, 60°, 90°, 120° and 150° of the bend and two extra fixations at the test section outlet. This flexible outer wall design allowed moderate adjustments of the flow field in the test section. It also allowed it to be replaced by another polycarbonate wall with a different shape, to give different free-stream boundary conditions. Both outer test section walls are shown in Fig. 1 the constant channel, which gave a zero pressure gradient flow and the converging channel, which gave a favourable pressure gradient flow.

A total number of five film injection configurations were investigated and are shown in Fig. 2. Injection configuration CONF 1 consisted of a row of nine cylindrical holes. The injection angle of the film holes was $\alpha = 30°$ relative to the surface. The holes were spaced three hole diameters in lateral direction, $P/D = 3.0$, and had a hole length-to-diameter ratio of $L/D = 7.5$. The second cylindrical injection geometry, CONF 2 had a lateral spacing of $P/D = 6.0$. Injection configuration CONF 3 consisted also of a row of 5 cylindrical holes, which were inclined at $\alpha = 30°$ to the surface and $\beta = 60°$ to the free-stream flow direction (compound angle). The lateral spacing of the holes was again $P/D = 6.0$. Injection configuration CONF 4 consisted of a row of five

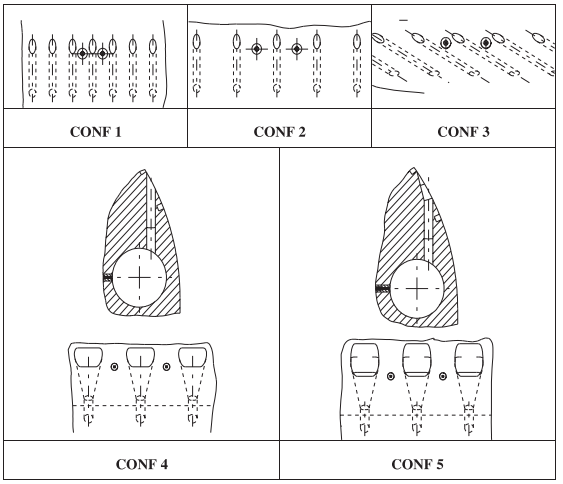


Fig. 2. Cylindrical and shaped film cooling hole geometries.

shaped holes, inclined at $\alpha = 30°$ to the test surface. The lateral spacing of the holes was $P/D = 6.0$, related to the throat diameter of the cylindrical entrance section of the shaped film holes. The cylindrical part of the hole channels had a length of 2.5 hole diameter. The remaining length, $L/D = 5.0$, of the hole channels were laterally opened. An outlet to inlet area ratio of $AR = 3.7$ was produced by the fan angle of $\varphi_1 = 12°$. Injection configuration CONF 5 had the same lateral extension angle $\varphi_1$ as CONF 4 and additionally a laid back angle $\varphi_2$. This streamwise widening of the film holes, $\varphi_2 = 15°$, was introduced further downstream of the cooling passages than the lateral widening and reduced the effective injection angle of the secondary fluid relative to the surface. Actually it was applied in the uncovered part of the cooling channels (see Fig. 2, CONF 5) and hence the effective area ratio was also $AR = 3.7$.

The surface temperature data were obtained by use of the narrow-band thermochromic liquid crystal technique. These measurement techniques were used for both adiabatic and heat transfer film cooling measurements. Isothermal temperature patterns on the test surface were indicated by narrow-band thermochromic liquid crystals and were observed by a colour image processing system. All additional experimental data, i.e., temperature, pressure and velocity information of the free-stream and secondary flow was recorded by a separate data acquisition system for later data reduction purposes.

During the adiabatic film cooling experiments the temperature indications of the thermochromic liquid crystals, $T_{TLC}$, were assumed to be the local adiabatic wall temperatures $T_{aw}$. With the additional information of the free-stream recovery $T_{r\infty}$ and secondary fluid total $T_c$ temperatures these isothermal contour lines were transformed into adiabatic film cooling effectiveness contours, $\eta_{ad}$,

$$\eta_{ad} = \frac{T_{r\infty} - T_{aw}}{T_{r\infty} - T_c}. \tag{1}$$

The recovery temperature of the free-stream flow was obtained for the turbulent external flow by using

$$T_{r\infty} = T_\infty + \left(Pr_\infty^{1/3} - 1\right)\frac{U_\infty^2}{2C_{p\infty}}. \tag{2}$$

In case of constant heat flux experiments with and without film cooling the thermochromic liquid crystal temperature, $T_{TLC}$, indicated the local wall temperatures $T_w$. For the measurements without film cooling the film cooling holes were covered with a thin aluminium tape to avoid additional sources of flow disturbances, that would increase heat transfer. The heat transfer coefficient in the absence of film cooling was calculated by

$$h_0 = \frac{\dot{q}_0}{T_{r\infty} - T_{rw}}, \tag{3}$$

where $\dot{q}_0$ is the constant heat flux without film cooling, created by electrical current send through the steel foil. Assuming that the electrical energy introduced into the steel foil was totally transformed into heat, due to foil resistance, $\dot{q}_0$ was determined from

$$\dot{q}_0 = R_{foil} I_{foil}^2, \tag{4}$$

where $R_{foil}$ is the specific foil resistance per unit area and $I_{foil}$ is the electrical current introduced into the foil. For the experiments with film cooling the heat transfer coefficients were defined by

$$h_f = \frac{\dot{q}_f}{T_{aw} - T_{rw}}, \tag{5}$$

where $\dot{q}_f$ is the constant heat flux with film cooling and $T_{aw}$ is the adiabatic wall temperature. For simplicity the heat transfer experiments were conducted at iso-energetic conditions ($T_c = T_\infty$). Further details of the used measurement method are given by Lutum et al. [17].

## 3. Results and discussion

Aerodynamic measurements without secondary fluid injection were conducted to determine the flow field quantities of the convex test section. Fig. 3 shows the isentropic free-stream Mach number distribution versus the streamwise distance. The coolant injection location corresponded to $S/D = 0$. It can be seen from the Mach number distribution that the free-stream is accelerated from $Ma_\infty \approx 0.18$ at $S/D = 0$ to $Ma_\infty \approx 0.65$ at $S/D \approx 35$. Further downstream the Mach number decreased almost linearly to the end of the test section. Care was taken in the experimental test design that the

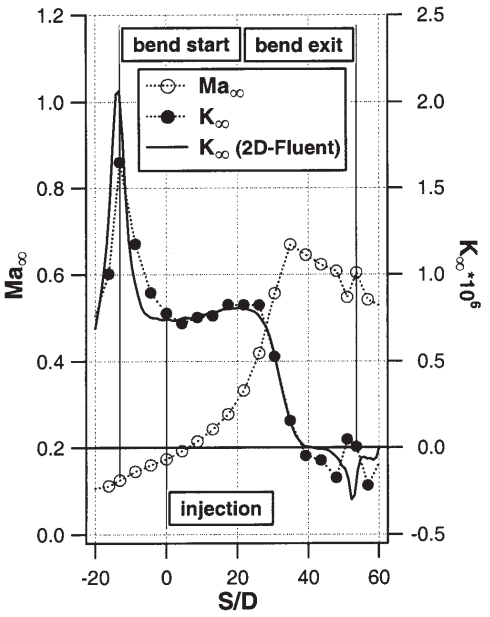


Fig. 3. Distributions of the free-stream Mach number and acceleration parameter versus streamwise distance.

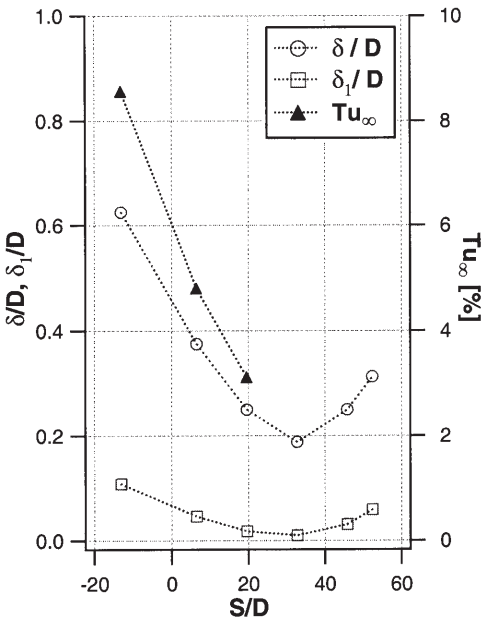


Fig. 4. Distributions of the boundary layer thickness, displacement thickness and local free-stream turbulence intensity versus streamwise distance.

flow did not separate in this area. Fig. 3 shows also the corresponding distribution of the acceleration parameter $K$ obtained from local static pressure measurements. The acceleration parameter $K$ is defined by

$$K = \frac{v_\infty}{U_\infty^2}\frac{\mathrm{d}U_\infty}{\mathrm{d}S}, \tag{6}$$

were $v_\infty$ and $U_\infty$ are the local free-stream viscosity and velocity values and $S$ is the streamwise coordinate.

Two-dimensional flow calculations were made in advance to find the proper geometrical shape of the outer wall. Corresponding results are also shown in Fig. 3. The desired constant acceleration parameter of about $K = 0.8E - 0.6$ was achieved inside the curved test section. It should be noted that the acceleration parameter is not constant over the whole distance of the test section. For streamwise distances larger than $S/D = 26$ the acceleration parameter decreased. At the end of the test section a deceleration occurred. Fig. 4 shows the thickness of the boundary layer and displacement layer normalised with the film hole diameter at different streamwise distances. The boundary layer thickness decreased with increasing streamwise distance until $S/D = 32$ due to free-stream acceleration. Further downstream, the acceleration parameter $K$ decreased and thus the boundary layer thickness values start to increase. At the injection location the boundary layer thickness was $\delta/D \approx 0.45$ and the displacement layer thickness $\delta_1/D \approx 0.065$. The local free-stream turbulence intensity is shown in Fig. 4. At the entrance of the curved test section it was about 8.5% and decreased due to free-stream acceleration with increasing streamwise distance. At the injection location a free-stream turbulence intensity of about 6% was obtained.

The density ratio was varied during the adiabatic experiments for injection configuration CONF 1 by using air and $CO_2$ as coolant fluids. A density ratio of DR $\approx 1.15$ was achieved during the adiabatic experiments with air-injection and DR $\approx 1.8$ with $CO_2$-injection. The results obtained with air-injection indicate a decreasing adiabatic film cooling effectiveness with increasing momentum flux ratio for streamwise distances $S/D \leqslant 20$ (Fig. 5). At a streamwise position $S/D = 40$ the results indicate first an increase and than a decrease in adiabatic film cooling effectiveness with increasing coolant mass flow. Highest film cooling effectiveness values were obtained at a momentum flux ratio close to one. The results obtained with $CO_2$-injection indicate in general an optimum adiabatic film cooling effectiveness value at a momentum flux ratio of $I \approx 0.5$. The results from injection configuration CONF 1 obtained with air- and $CO_2$-injection correlated quite well with the momentum flux ratio. The adiabatic film cooling effectiveness of injection configuration CONF 2 is about 50% lower than the corresponding values from injection configuration CONF 1, which corresponds to the different hole spacing for these two injection configurations ($P/D_{\mathrm{CONF1}} = 3$ and $P/D_{\mathrm{CONF2}} = 6$). This effect is shown in Fig. 5.

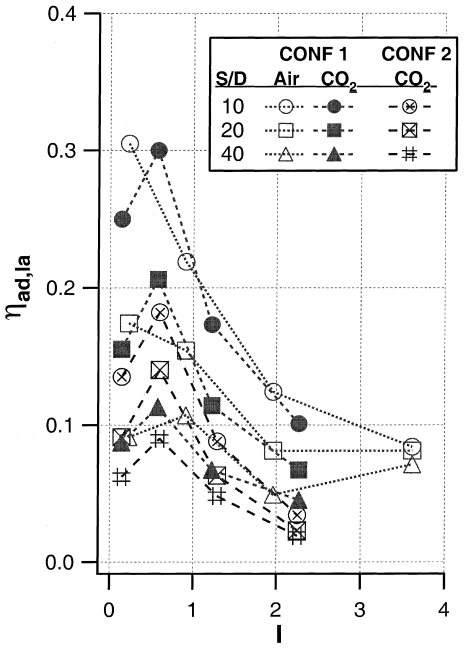


Fig. 5. Distributions of lateral averaged film cooling effectiveness values versus momentum flux ratio for different streamwise positions (air and $CO_2$ injection, $R/D = 25$).

Fig. 6 compares lateral averaged film cooling effectiveness results obtained for cylindrical (CONF 2 and CONF 3) and shaped (CONF 4 and CONF 5) holes at different blowing rates $M = 0.5$, 1.0, 1.5 and 2.0 for $CO_2$-injection. Injection configuration CONF 3 indicates a weaker dependence on the investigated blowing rates than the corresponding results for CONF 2. Especially at higher blowing rates higher film cooling effectiveness values were achieved by CONF 3 due to the compound coolant injection compared to CONF 2. All injection configurations with cylindrical holes indicate an optimum film cooling effectiveness within the investigated range of blowing rate at about $M = 1$. The results obtained with the shaped injection configurations CONF 4 and CONF 5 indicate in general increasing adiabatic film cooling effectiveness with increasing blowing rates. This can be attributed to the reduced momentum of the coolant flow at the hole exit due to hole extension. The hole extension in lateral direction improved also the lateral spreading of the coolant fluid on the surface to be cooled. The highest benefit of the shaped holes occurs for blowing rates of $M > 1$. Results obtained with injection configuration CONF 5, the laid back shaped holes, indicate a stronger decay of the lateral averaged film cooling effectiveness than for CONF 4. Fig. 7 shows the lateral averaged values for the adiabatic film cooling effectiveness as a function of the blowing rate at two streamwise locations. The different sensitivity to the blowing rate for the two types of injection configurations can be seen clearly. The shaped injection configurations show better film cooling effectiveness values at higher blowing rates in comparison to the cylindrical injection configurations. The cylindrical injection configuration CONF 2 indicates decreasing film cooling effectiveness values for blowing rates of $M > 1$.

As the heat transfer coefficient is dependent on the free-stream velocity and properties of the secondary fluid, it is difficult to compare the heat transfer performance for experiments conducted for different free-stream boundary conditions. Therefore the heat transfer data will be presented here as Stanton numbers. The Stanton number is defined by

$$St_f = \frac{h_f}{c_{p,f}\,\rho_f U_\infty}, \tag{7}$$

were $h_f$ and $U_\infty$ are the local values for the heat transfer coefficient and the free-stream velocity, respectively. In the case of $CO_2$ injection the values for the specific heat $c_{p,f}$ and density $\rho_f$ are changing in streamwise direction because of the mixing between the coolant and free-stream fluids. To calculate adequate values for $c_{p,f}$ and $\rho_f$, the results for the adiabatic film cooling effectiveness determined at the same blowing rate were used. The mixing of $CO_2$ and the free-stream air is then calculated by applying the analogy of heat and mass transfer [18]. With this analogy the film cooling effectiveness can be expressed in terms of a concentration ratio of coolant to free-stream for incompressible flows

$$\eta_{ad} = \frac{T_{r\infty} - T_{aw}}{T_{r\infty} - T_c} = \frac{C_\infty^{CO_2} - C_w^{CO_2}}{C_\infty^{CO_2} - C_c^{CO_2}} = C_w^{CO_2}. \tag{8}$$

With the $CO_2$ concentrations in the free-stream ($C_\infty^{CO_2} = 0$) and in the coolant ($C_c^{CO_2} = 1$) the local $CO_2$ concentration at the wall ( $C_w^{CO_2}$) can be directly estimated from the local adiabatic film cooling effectiveness values. The local fluid properties of the air/$CO_2$-mixture can thus be determined to calculate the correct Stanton numbers.

Heat transfer experiments with injection configuration CONF 1 were conducted with air and $CO_2$ as coolant. The coolant and free-stream temperatures were adjusted to the same level during these experiments. Therefore a density ratio of DR = 1.0 was obtained for air-injection and a density ratio of DR = 1.53 with $CO_2$-injection was obtained. Fig. 8 shows lateral averaged Stanton number ratios obtained with air and $CO_2$ injection versus the momentum flux ratio for injection configuration CONF 1. The heat transfer increase due to coolant injection is more pronounced for air-injection for streamwise distances $S/D \leqslant 20$. Further downstream ($S/D = 40$) no significant differences can be observed between air and $CO_2$-injection. The results obtained with $CO_2$-injection for CONF 2 indicate generally less or similar heat transfer increase due to coolant injection

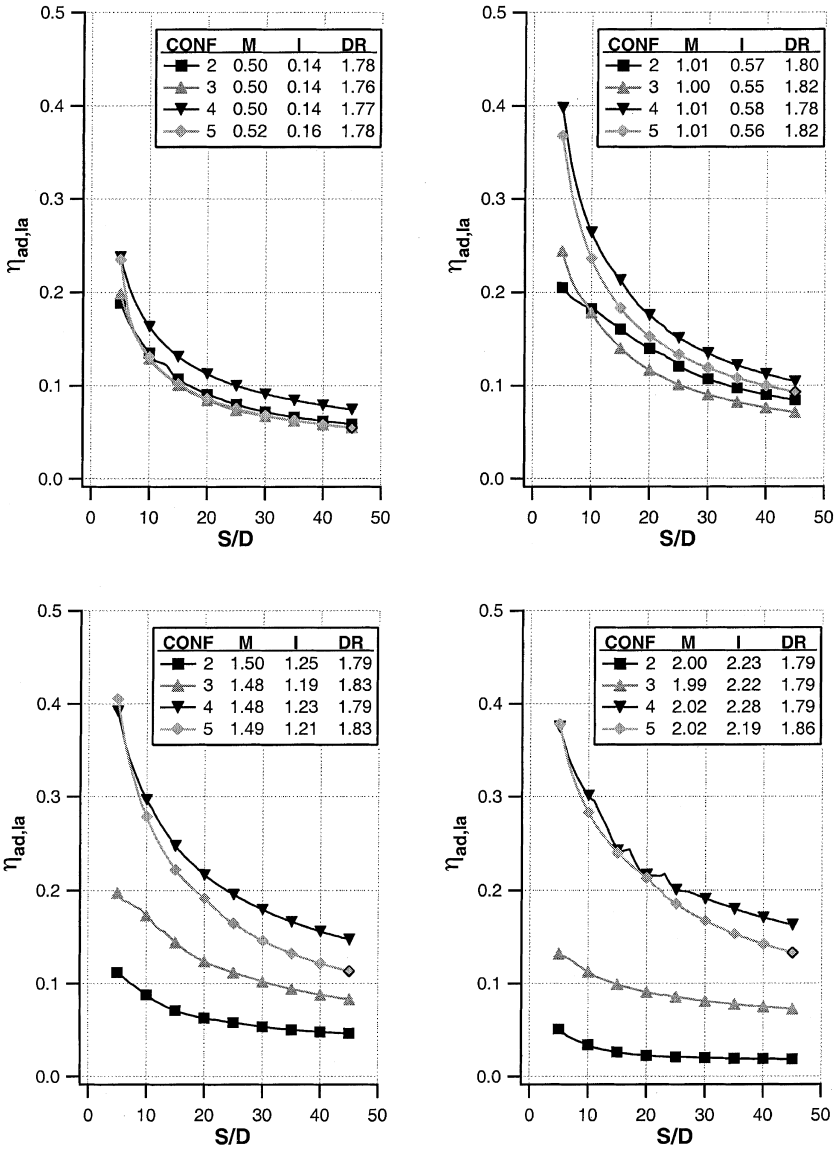


Fig. 6. Distributions of lateral averaged film cooling effectiveness values versus streamwise distance for different blowing rates ($CO_2$ injection, $R/D = 25$).

than CONF 1. At high coolant mass flows the reduction in heat transfer increase due to the larger hole spacing (CONF 1: $P/D = 3$ and CONF 2: $P/D = 6$) was especially obvious.

Fig. 9 compares lateral averaged Stanton number ratios obtained for cylindrical (CONF 2 and 3) and shaped (CONF 4 and 5) injection configurations at different coolant blowing rates of $M = 0.5$ and $M = 2.0$ using $CO_2$-injection. The heat transfer ratios obtained for cylindrical holes increase with growing blowing rate. The heat transfer ratios obtained with CONF 3 are slightly higher than those obtained with CONF 2. The heat transfer results obtained for the shaped injection configurations indicate very little sensitivity to the blowing rate. This is attributed to the reduction in coolant exit momentum due to the hole extension. The reduced coolant exit momentum caused less flow disturbance of the free-stream flow and lead therefore to less heat transfer increase even at high blowing rates. There is a quite strong increase in heat transfer due to coolant injection from injection configuration CONF 5 close to the injection location. This could have been caused by a local flow separation within or just downstream of these laid back shaped holes. However, this increased heat transfer vanished rapidly with downstream distance. The results obtained further

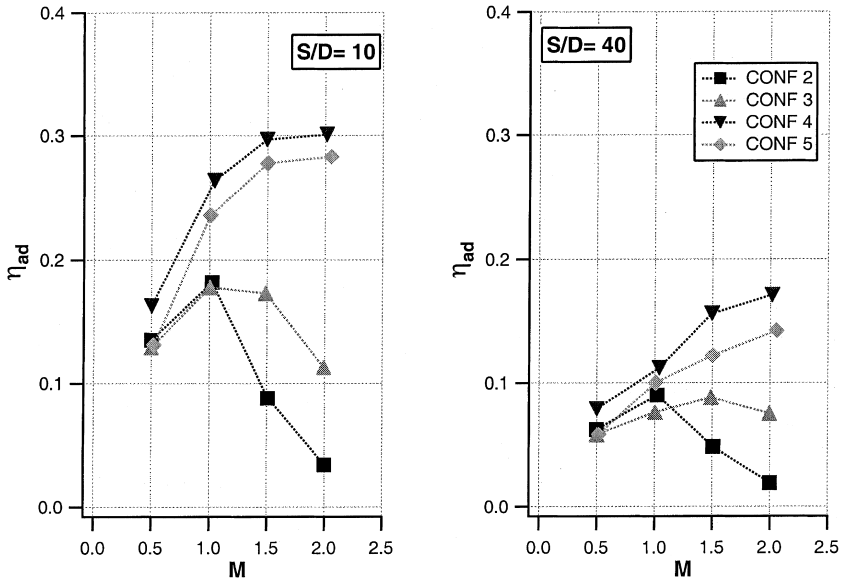


Fig. 7. Distributions of lateral averaged film cooling effectiveness values versus blowing rate for different streamwise positions ($CO_2$ injection, $R/D = 25$).

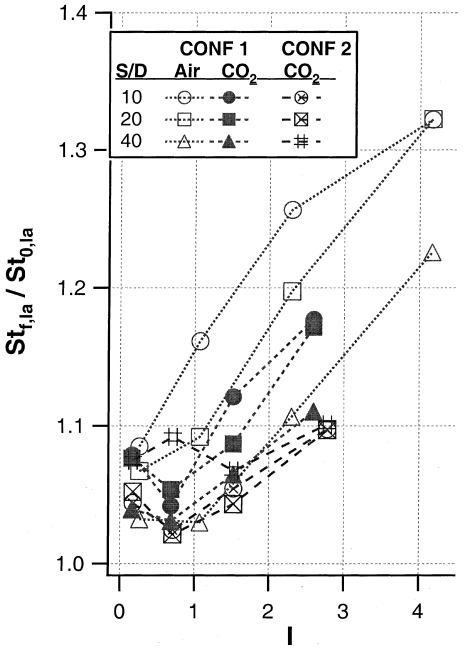


Fig. 8. Distributions of lateral averaged Stanton number ratios versus momentum flux ratio for different streamwise positions (air and $CO_2$ injection, $R/D = 25$).

downstream ($S/D > 25$) indicate the lowest heat transfer ratios from all injection configurations investigated. The heat transfer ratios shown in Fig. 9 indicate a distinct increase for $S/D > 30$, which was attributed to the change of the free-stream pressure gradient. The range of constant free-stream acceleration finished at $S/D \approx 25$. Further downstream the flow acceleration decreased and a slight deceleration occurred for $S/D > 35$. The increase in heat transfer is generally small. The variation of the Stanton number ratio with the blowing rate is stronger for injection with cylindrical holes then with shaped holes. By using shaped holes, the increase in heat transfer is almost constantly for varying blowing rates and less than 10%.

## 4. Influence of free-stream acceleration

The current results obtained for an accelerated free-stream are compared with previous results obtained with constant free-stream velocity [17]. The same experimental facility and the same injection configurations were used to determine both adiabatic film cooling effectiveness values and heat transfer coefficient for the different free-stream flow conditions (see Fig. 1). By comparing the data for each injection configuration at the same blowing rates, the influence of the free-stream acceleration on the film cooling performance can be determined. The lateral averaged adiabatic film cooling effectiveness for each blowing rate obtained for an accelerated free-stream is related to the film cooling effectiveness obtained for constant free-stream velocity. This ratio shows the influence of the different free-stream boundary conditions. Values above one indicate increasing film cooling effectiveness and values below one indicate decreasing values due to the accelerated free-stream.

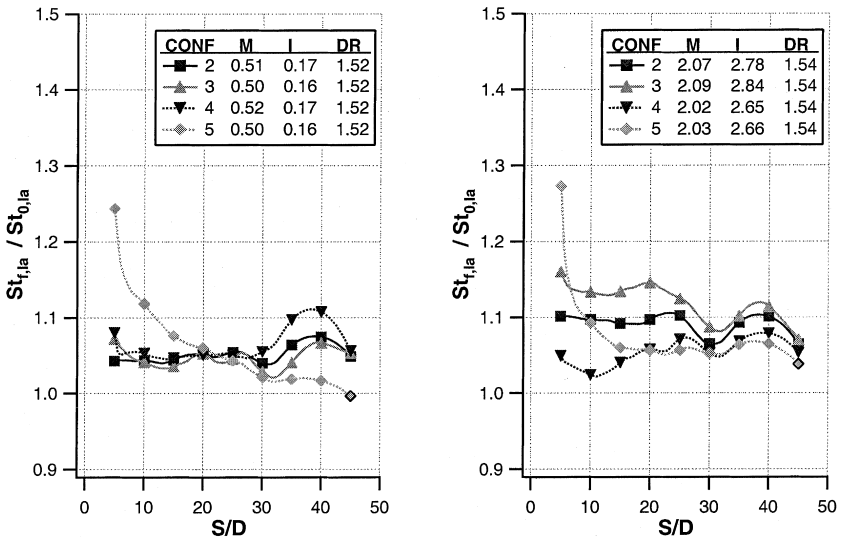


Fig. 9. Distributions of lateral averaged Stanton number ratios versus streamwise distance for different blowing rates ($CO_2$ injection, $R/D = 25$).

Fig. 10 shows the influence of free-stream acceleration on the ratios of film cooling effectiveness obtained for CONF 2, CONF 3, CONF 4 and CONF 5 for $CO_2$-injection. In general, it can be seen that the free-stream acceleration causes a decrease in film cooling effectiveness. This decrease is more pronounced with increasing streamwise distance. At the end of the test section, the film cooling effectiveness was lowered by about 20–40% depending on the blowing rate and injection configuration. The decrease in film cooling effectiveness was generally stronger for cylindrical holes than for the shaped injection configurations. In the near hole region the film cooling effectiveness of CONF 2 was increased for moderate and high blowing rates. The maximum increase was about 20% for a blowing rate of $M = 1.5$. The increased effectiveness in the case of accelerated free-stream might be caused by the suppression of jet separation at higher blowing rates. Due to the free-stream acceleration, the injected coolant might be pushed more towards the surface, which causes higher film cooling effectiveness values close to the injection position compared to the case with constant free-stream velocity. In contrast to CONF 2 the increase of effectiveness in the near hole region due to acceleration is nearly not visible for injection configuration CONF 3. As the effect of jet separation was found to be less important for injection configuration CONF 3, the positive influence of a free-stream acceleration on the jet separation process is also less important. Film cooling effectiveness ratios obtained with injection configuration CONF 4 indicated a 5–10% increase in the near hole region for lower blowing rates ($M = 0.5$ and 1.0) due to free-stream acceleration. The distributions for the higher blowing rates ($M = 1.5$ and 2.0) show little sensitivity with streamwise distance. The film cooling effectiveness ratios for injection configuration CONF 5 indicate no increase of effectiveness in the near hole region. The free-stream acceleration causes a stronger decrease in film cooling effectiveness results obtained with CONF 5 compared to those of CONF 4.

Hartnett et al. [1] presented a scaling method for the adiabatic film cooling effectiveness to account for the influence of the pressure gradient

$$\eta^*_{\mathrm{ad,la}}(S/D) = \eta_{\mathrm{ad}}(S/D)\left[\frac{U_\infty(S/D)}{U_\infty(S/D=0)}\right]^{\alpha}, \quad \alpha = 0.2. \quad (9)$$

The lateral averaged adiabatic film cooling effectiveness distribution $\eta_{\mathrm{ad,la}}(S/D)$ obtained with free-stream acceleration was modified by the ratio of the local free-stream velocity $U_\infty(S/D)$ to the free-stream velocity at coolant injection $U_\infty(S/D = 0)$. The exponent $\alpha = 0.2$ was determined from their experimental results for a slot injection on a flat plate. This scaling method was applied to the current results obtained with CONF 2 and CONF 4. A least square method was used to determine the exponent for the cylindrical and shaped hole results separately. Fig. 11 shows the present results (left) and the scaled distributions (right) obtained with injection configuration CONF 2. The exponent $\alpha$ was calculated as 0.24 for the cylindrical holes. Results obtained with injection configuration CONF 4 indicate a lower decrease in film cooling effectiveness and hence the exponent was decreased to 0.15 (Fig. 12). It can be concluded that the scaling method proposed by Hartnett et al. [1] accounts quite well for the acceleration effect on adiabatic film cooling effectiveness.

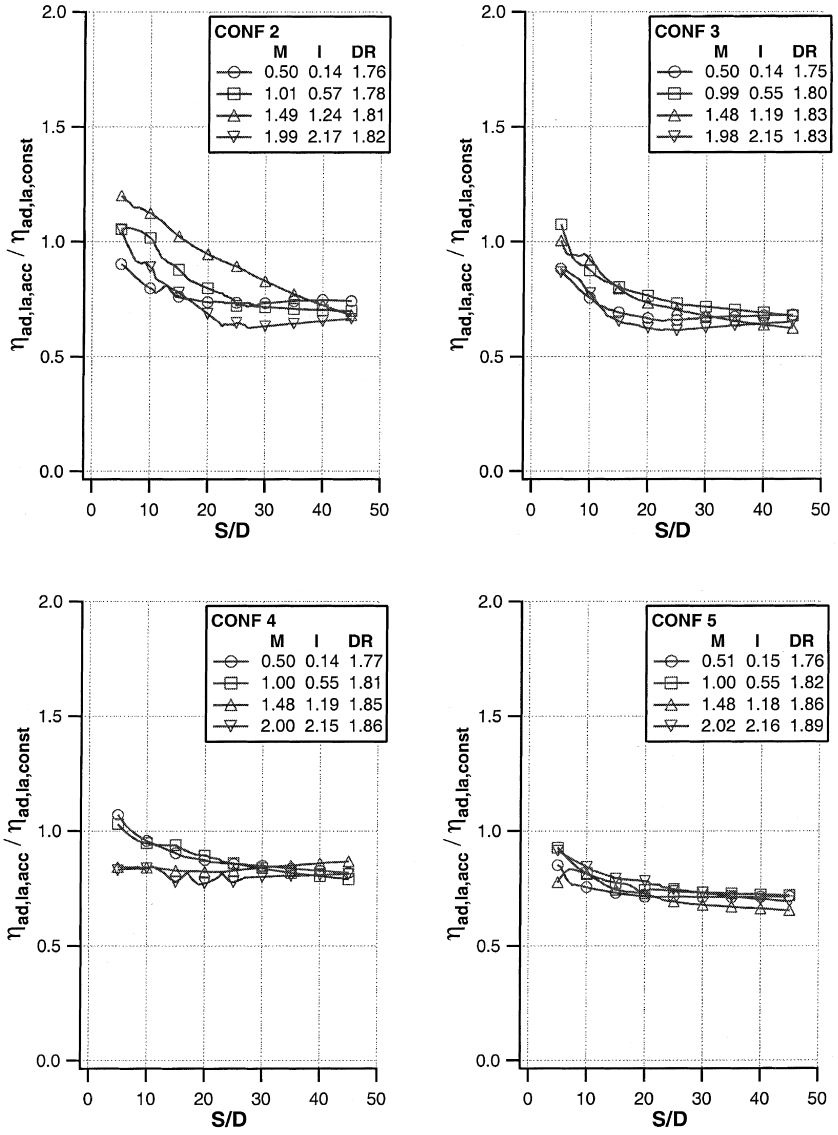


Fig. 10. Effect of free-stream acceleration on lateral averaged adiabatic film cooling effectiveness values versus streamwise distance for different blowing rates ($CO_2$ injection, $R/D = 25$).

To consider the combined effect of acceleration on the adiabatic film cooling effectiveness and the heat transfer, the heat flux ratios with and without film cooling should be investigated. The ratio of the heat fluxes with and without film cooling can be expressed with Eqs. (3) and (5) as

$$\frac{\dot{q}_f}{\dot{q}_0} = \frac{h_f}{h_0}\frac{(T_{aw} - T_w)}{(T_{r\infty} - T_w)}. \tag{10}$$

With the definition of the adiabatic film cooling effectiveness and a dimensionless wall temperature $\Theta$ this ratio can be expressed for a defined wall temperature as

$$\frac{\dot{q}_f}{\dot{q}_0} = \frac{h_f}{h_0}(1 - \eta_{ad}\Theta), \tag{11}$$

where $\Theta$ is defined as

$$\Theta = \frac{T_{r\infty} - T_c}{T_{r\infty} - T_w}. \tag{12}$$

Here $\Theta$ describes the boundary conditions of the cooling process. By setting a reasonable value for $\Theta$, with the determined values for the adiabatic film cooling effectiveness and the heat transfer coefficient, the heat flux ratio $\dot{q}_f/\dot{q}_o$ can easily be calculated. As the ratio $\dot{q}_f/\dot{q}_o$ is

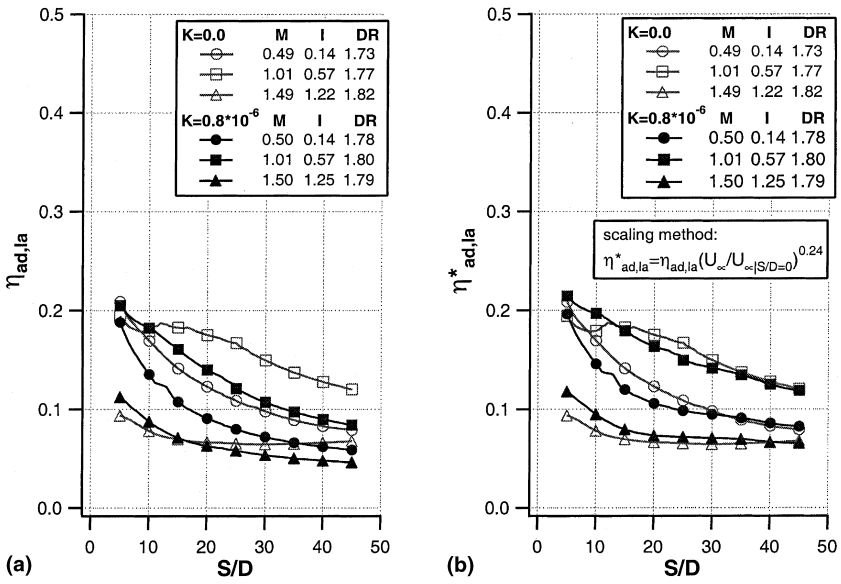


Fig. 11. Effect of free-stream acceleration on lateral averaged adiabatic film cooling effectiveness values versus streamwise distance for different blowing rates (CONF 2, $CO_2$ injection, $R/D = 25$; (a): present results; (b): scaled results with method by Hartnett et al. [1]).

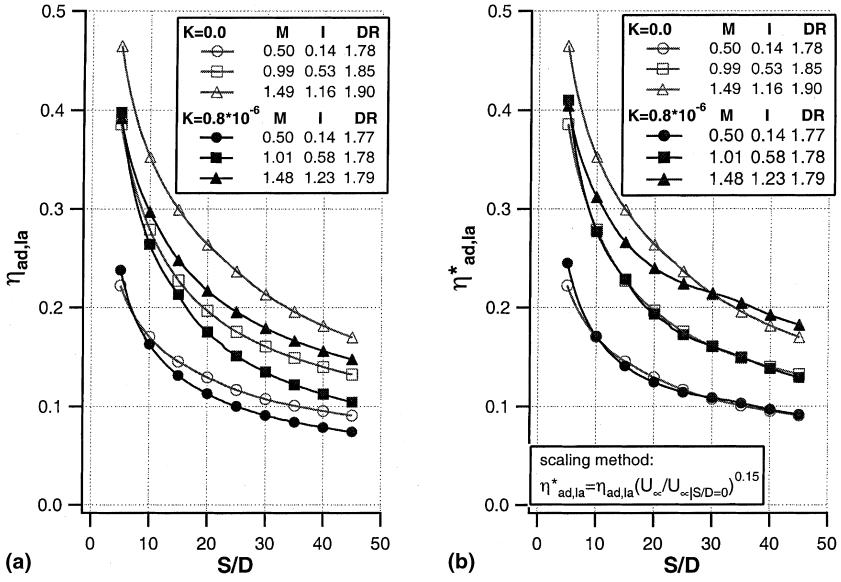


Fig. 12. Effect of free-stream acceleration on lateral averaged adiabatic film cooling effectiveness values versus streamwise distance for different blowing rates (CONF 4, $CO_2$ injection, $R/D = 25$; (a): present results; (b): scaled results with method by Hartnett et al. [1]).

different for each injection configuration and varies with the blowing rate it can be seen as an indicator of the film cooling quality at a certain blowing rate. Heat flux ratios below 1 indicate a reduction of the heat flux into the surface that needs to be cooled. Heat flux ratios above 1 indicate that the film cooling process increases the heat flux into the surface compared to the case without film cooling.

Distributions of heat flux ratios are shown in Fig. 13 for the different injection configurations for the investigated blowing rates. It can be seen that the free-stream acceleration has a negative effect on the film cooling performance.

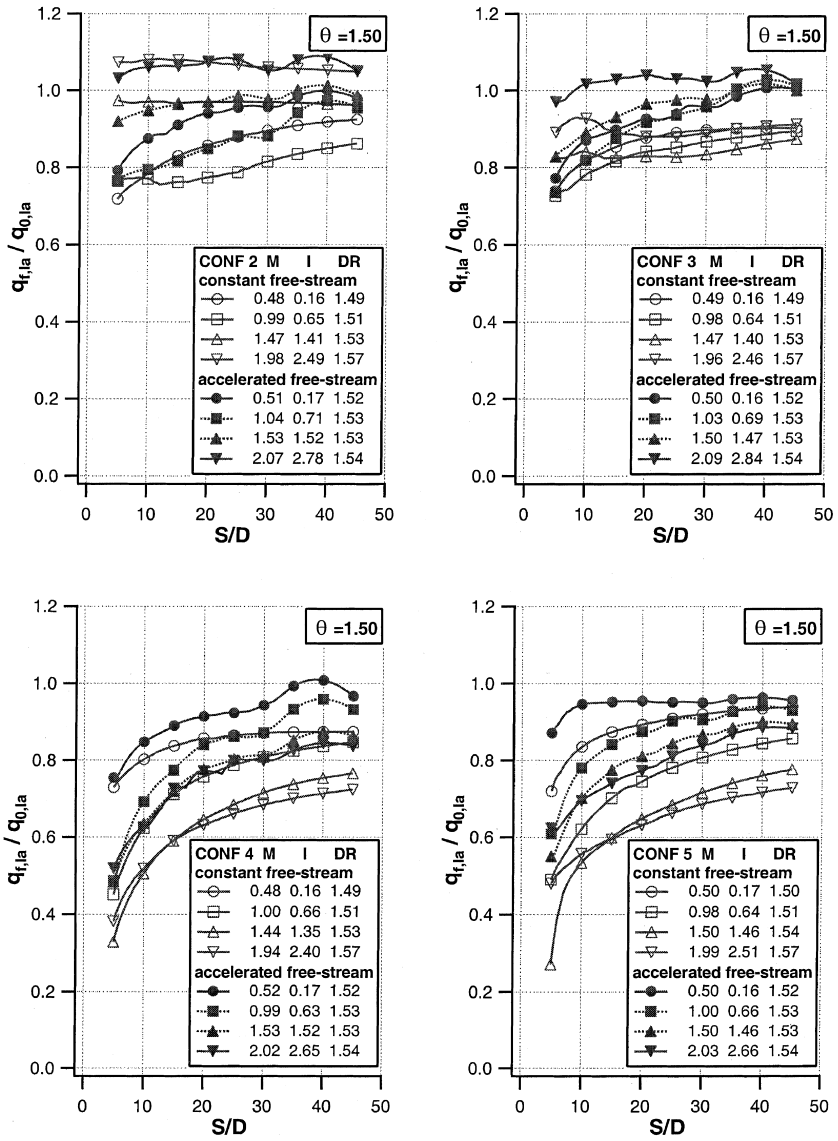


Fig. 13. Distributions of lateral averaged heat flux ratios versus streamwise distance for constant and accelerated free-stream flow and different blowing rates ($CO_2$ injection, $R/D = 25$).

The heat flux reduction due to film injection is less for the case with free-stream acceleration compared to the case of constant free-stream velocity. The reduction in overall film cooling performance due to free-stream acceleration is about 10–20% depending on injection configuration and blowing rate. Furthermore it can be observed that shaped film cooling holes achieve highest film cooling performance at high blowing rates. The cylindrical injection configurations show for higher blowing rates the interesting effect that coolant injection results in an increasing heat flux compared to the case without film cooling. Therefore, film cooling should not be applied in such a situation.

## 5. Conclusion

In the present study, the film cooling performance on a convex test surface with favourable free-stream pressure gradient was investigated. The test section had a ratio of surface curvature radius to film hole diameter of $R/D = 25$. The free-stream follows a 150°-bend in the test section, with secondary fluid ($CO_2$ or air) injected at a bend angle of $\gamma_{inj} = 30°$. Five different injection configurations were investigated during this film cooling test program. The multiple narrow-band thermochromic liquid crystal wall surface temperature measurement

technique was used for the measurement of the adiabatic film cooling effectiveness and heat transfer coefficient. The current experiments were conducted with an increased free-stream turbulence intensity of about $Tu_\infty = 6\%$ at coolant injection. Aerodynamic measurements were conducted to determine the flow field along the convex test surface. Distributions of the boundary layer thickness and free-stream turbulence intensities were determined by hot-wire traverses.

The film cooling results obtained with favourable pressure gradient along a convex test surface indicate that shaped holes provide higher adiabatic film cooling effectiveness values, especially for blowing rates $M > 1.0$. An increase in blowing rate in the range of $0.5 < M < 2.0$ resulted in an increased adiabatic film cooling effectiveness. The adiabatic film cooling effectiveness results obtained for cylindrical holes show decreasing values for higher blowing rates because of coolant jet separation. Jet separation occurred on the convex surface for momentum flux ratios $I > 0.6$. In general a moderate increase in heat transfer due to film injection was observed. The heat transfer increase with $CO_2$ injection was found to be less than with air injection. Stanton number ratios obtained with cylindrical holes indicated a higher sensitivity with blowing rate.

A favourable pressure gradient caused in general decreasing adiabatic film cooling effectiveness far downstream compared to the case with zero pressure gradient flow. This reduction was of the magnitude of 20–40% depending on injection configuration and blowing rate. In the near hole region an increase in film cooling effectiveness could occur due to free-stream acceleration. The influence of the free-stream acceleration on heat transfer with film injection was in general small. The film cooling performance, respectively the heat flux ratio with and without film injection was reduced by free-stream acceleration. This was attributed to decreasing film cooling effectiveness values and slightly increased heat transfer due to the free-stream acceleration.

## Acknowledgements

This work was carried out within the Brite EuRam project "Turbine Aero-Thermal External Flows" (BE97-4440) and was sponsored by the Bundesamt für Bildung und Wissenschaft (Switzerland). The authors wish to acknowledge the fruitful collaboration with their partners within this project and their permission to publish this paper. Additionally the authors would like to thank ABB ALSTOM POWER for the permission to publish the paper.

## References

[1] J.P. Hartnett, R.C. Birkebak, E.R.G. Eckert, Velocity distributions, temperature distributions effectiveness and heat transfer in cooling of a surface with a pressure gradient, International Development in Heat Transfer, Part 4, ASME (1961) 682–689.

[2] R.A. Seban, L.H. Back, Effectiveness and heat transfer for a turbulent boundary layer with tangential injection and variable free-stream velocity, J. Heat Transfer 84 (1962) 235–244.

[3] L.W. Carlson, E. Talmor, Gaseous film cooling at various degrees of hot gas acceleration and turbulence levels, Int. J. Heat Mass Transfer 11 (1968) 1695–1713.

[4] M.P. Escudier, J.H. Whitelaw, The Influence of strong adverse pressure gradients on the effectiveness of film cooling, Int. J. Heat Mass Transfer 11 (1968) 1289–1292.

[5] B.R. Pai, J.W. Whitelaw, The Influence of strong pressure gradients on film cooling effectiveness, Heat Transfer 2 (1970).

[6] B.E. Launder, J. York, Discrete-hole cooling in the presence of free stream turbulence and strong favourable pressure gradient, Int. J. Heat Mass Transfer 17 (1974) 1403–1409.

[7] M.Y. Jabbari, R.J. Goldstein, Effect of free-stream acceleration on adiabatic wall temperature and heat transfer downstream of gas injection, in: Proceedings of the Sixth International Heat Transfer Conference, vol. 5, 1978, pp. 249–254.

[8] H. Kruse, Effects of hole geometry, wall curvature and pressure gradient on film cooling downstream of a single row, propulsion and energetics panel, in: Symposium, vol. 65, Bergen, 1985, AGARD Conference Proceedings, vol. 390, 1985, pp. 8.1–8.13.

[9] N. Hay, D. Lampard, C.L. Saluja, Effects of cooling films on the heat transfer coefficient on a flat plate with zero mainstream pressure gradient, J. Eng. Gas Turbines Power 107 (1985) 99–104.

[10] H.D. Ammari, N. Hay, D. Lampard, Effect of acceleration on the heat transfer coefficient on a film-cooled surface, J. Turbomachinery 113 (1991) 464–471.

[11] M. Sivrioglu, An analysis of the effects of pressure gradient and streamline curvature on film cooling effectiveness, Wärme-und Stoffübertragung 26 (1991) 103–107.

[12] F.E. Ames, Aspects of vane film cooling with high turbulence: Part 1 – heat transfer, ASME Paper 97-GT-239 (1997).

[13] F.E. Ames, Aspects of vane film cooling with high turbulence: Part 2 – adiabatic effectiveness, ASME Paper 97-GT-240 (1997).

[14] U. Drost, and A. Bölcs, Performance of a turbine airfoil with multiple film cooling stations. Part I: heat transfer and film cooling effectiveness, ASME Paper 99-GT-171 (1999).

[15] J.D. Heidmann, D.L. Rigby, A.A. Ameri, A three-dimensional coupled internal/external simulation of a film-cooled turbine vane, ASME Paper 99-GT-186 (1999).

[16] L. Zhang, M. Baltz, R. Pudupatty, M. Fox, Turbine nozzle film cooling study using the pressure sensitive paint (PSP) technique, ASME Paper 99-GT-196 (1999).

[17] E. Lutum, J. von Wolfersdorf, B. Weigand, K. Semmler, Film cooling on a convex surface with zero pressure gradient flow, International J. Heat Mass Transfer (accepted).

[18] J.N. Shadid, E.R.G. Eckert, The mass transfer analogy to heat transfer fluids with temperature-dependent properties, J. Turbomachinery 113 (1991).